NASA TECHNICAL NOTE

NASA TN D-5433

c. 1

NASA TN D-5433

COMPARISON OF PREDICTION METHODS AND STUDIES OF RELAXATION IN HYPERSONIC TURBULENT NOZZLE-WALL BOUNDARY LAYERS

by Dennis M. Bushnell, Charles B. Johnson, William D. Harvey, and William V. Feller

Langley Research Center
Langley Station, Hampton, Va.

NATIONAL AERONAUTICS AND SPACE ADMINISTRATION • WASHINGTON, D. C. • SEPTEMBER 1969

1. Report No. NASA TN D-5433	2. Government Accession No.
3. Recipient's Catalog No.	
4. Title and Subtitle COMPARISON OF PREDICTION METHODS AND STUDIES OF RELAXATION IN HYPERSONIC TURBULENT NOZZLE-WALL BOUNDARY LAYERS	5. Report Date September 1969
	6. Performing Organization Code
7. Author(s) Dennis M. Bushnell, Charles B. Johnson, William D. Harvey, and William V. Feller	8. Performing Organization Report No. L-6578
9. Performing Organization Name and Address NASA Langley Research Center Hampton, Va. 23365	10. Work Unit No. 129-01-20-07-23
	11. Contract or Grant No.
12. Sponsoring Agency Name and Address National Aeronautics and Space Administration Washington, D.C. 20546	13. Type of Report and Period Covered Technical Note
	14. Sponsoring Agency Code

15. Supplementary Notes

This report was one of the papers presented at the Symposium on Compressible Turbulent Boundary Layers, Langley Research Center, Dec. 10-11, 1968.

16. Abstract

Recent turbulent boundary-layer measurements on axisymmetric nozzle walls at Mach numbers of 6, 8, and 19 are presented and compared with the predictions of two theoretical methods. One of the methods was of the integral type; the other was a finite-difference solution to the governing differential equations. The integral method gave good predictions of the data at Mach 6 and 8 and a reasonable prediction at Mach 19. Results for the finite-difference approach were available only at Mach 8, for which good agreement with data was obtained.

A survey of boundary-layer data indicates that the variation of total temperature with velocity for flat-plate type of flows can be represented within the scatter of the data by the linear Crocco relation, whereas for nozzle-wall flows, this relation is generally more nearly quadratic. A finite-difference solution for the Mach 8 nozzle-wall boundary layer resulted in a quadratic-type temperature-velocity relation in the strong favorable pressure-gradient region downstream of the throat. However, near the nozzle exit the theoretical solution tended to approach the linear variation of Crocco. Apparently, the observed quadratic variation in nozzle boundary layers can be at least partly accounted for by the pressure-gradient history of the flow.

17. Key Words Suggested by Author(s) Turbulent boundary layer; Relaxation; Turbulence; Nozzle-wall flow	18. Distribution Statement Unclassified – Unlimited

19. Security Classif. (of this report)	20. Security Classif. (of this page)	21. No. of Pages	22. Price*
Unclassified	Unclassified	33	$3.00

*For sale by the Clearinghouse for Federal Scientific and Technical Information
Springfield, Virginia 22151

COMPARISON OF PREDICTION METHODS AND STUDIES OF RELAXATION IN HYPERSONIC TURBULENT NOZZLE-WALL BOUNDARY LAYERS*

By Dennis M. Bushnell, Charles B. Johnson,
William D. Harvey, and William V. Feller
Langley Research Center

SUMMARY

Recent turbulent boundary-layer measurements on axisymmetric nozzle walls at Mach numbers of 6, 8, and 19 are presented and compared with the predictions of two theoretical methods. One of the methods was of the integral type; the other was a finite-difference solution to the governing differential equations. The integral method gave good predictions of the data at Mach 6 and 8 and a reasonable prediction at Mach 19. Results for the finite-difference approach were available only at Mach 8, for which good agreement with data was obtained.

A survey of boundary-layer data indicates that the variation of total temperature with velocity for flat-plate type of flows can be represented within the scatter of the data by the linear Crocco relation, whereas for nozzle-wall flows, this relation is generally more nearly quadratic. A finite-difference solution for the Mach 8 nozzle-wall boundary layer resulted in a quadratic-type temperature-velocity relation in the strong favorable pressure-gradient region downstream of the throat. However, near the nozzle exit the theoretical solution tended to approach the linear variation of Crocco. Apparently, the observed quadratic variation in nozzle boundary layers can be at least partly accounted for by the pressure-gradient history of the flow.

Profile measurements along a straight pipe extension downstream of the nozzle exit of the Mach 6 tunnel indicate that at a distance of the order of 60 boundary-layer thicknesses, the flow tended to relax toward the linear temperature-velocity variation.

INTRODUCTION

Because of the difficulty of obtaining fully developed turbulent boundary-layer flows on flat plates and hollow cylinders at hypersonic speeds (ref. 1), turbulent boundary layers

*This report was one of the papers presented at the Symposium on Compressible Turbulent Boundary Layers, Langley Research Center, Dec. 10-11, 1968.

on nozzle walls have been surveyed extensively. Also, more accurate measurements can be obtained on tunnel-wall boundary layers because of their comparatively larger thickness. There have been only a limited number of comparisons made between the measured profiles and integral thicknesses with the results of theoretical methods wherein the nozzle pressure-gradient history is taken into account. (See, for example, refs. 2, 3, and 4.) Therefore, there is some question as to the magnitude of the effects of the favorable pressure-gradient history on the profiles measured at the nozzle exit. That is, because of past history, the boundary layer at the nozzle exit (where the pressure gradient is usually small locally) may not have the same characteristics as a boundary layer which developed in a zero-pressure-gradient situation.

On the basis of skin-friction and heat-transfer data obtained on both a flat plate and a tunnel wall, Wallace (ref. 5) concluded that the two flows tend to have a close correspondence as far as surface phenomena are concerned. However, discussion in references 6, 7, and 8 (based on limited profile measurements) indicates that the temperature and velocity profiles for the nozzle-wall boundary layer are appreciably different from those for the flat-plate case.

The purpose of this paper is to present some recent nozzle-wall turbulent-boundary-layer measurements at Mach numbers of 6, 8, and 19, and to compare the results obtained with two theories which utilize the upstream pressure history in computing the flow. One of the theories is of the conventional integral type, and the assumptions used are examined as to relative applicability in flat-plate and nozzle flows. The other approach is a nonsimilar numerical solution of the governing differential equations and hence should be able to give an indication of the effects of the upstream favorable pressure gradient on the profiles at the nozzle exit. Numerical procedures for solving the differential equations have previously been developed by A. M. O. Smith (ref. 9) and others.

SYMBOLS

A	constant in eddy viscosity expression (eq. (4))
c_p	specific heat
C_f	skin-friction coefficient
H	total enthalpy
H^*	form factor, δ^*/θ

l	mixing length (eq. (4))
M	Mach number
N	index in velocity profile (eq. (6))
p	pressure
N_{Pr}	Prandtl number
$N_{Pr,t}$	turbulent Prandtl number
R	Reynolds number
r	radius
T	temperature
u,v	velocity components in x- and y-directions, respectively
x,y	Cartesian coordinates along and normal to surface, respectively
α	exponent in total-temperature-velocity relationship (eq. (5))
ρ	density
ϵ	eddy viscosity
κ	eddy conductivity
μ	viscosity
τ	shear stress
δ	boundary-layer thickness taken where $\frac{u}{u_e} = 0.995$
δ^*	displacement thickness
θ	momentum thickness

$$\bar{\theta} = \frac{T_t - T_w}{T_{t,\infty} - T_w}$$

Subscripts:

t	total
w	wall
∞	local free stream
e	local external to boundary layer

A prime denotes a fluctuating quantity.

DESCRIPTION OF THEORIES

Finite-Difference Approach

The finite-difference method solves the compressible turbulent-boundary-layer equations in terms of mean flow quantities (ref. 10). With the following assumptions for the Reynolds stress and heat transfer

$$-\rho\,\overline{u'v'} = \epsilon\,\frac{\partial u}{\partial y}$$

$$-\rho\,\overline{v'T'} = \kappa\,\frac{\partial T}{\partial y}$$

and the definition of turbulent Prandtl number

$$\frac{c_p \epsilon}{\kappa} = N_{Pr,t}$$

the governing equations become

For continuity:

$$\frac{\partial}{\partial x}\left(\rho u r^j\right) + \frac{\partial}{\partial y}\left(\rho v r^j\right) = 0 \qquad (1)$$

where $j = 1$ for axisymmetric flows and $j = 0$ for two-dimensional flows

For conservation of momentum:

$$\rho u \frac{\partial u}{\partial x} + \rho v \frac{\partial u}{\partial y} = -\frac{dp}{dx} + \frac{\partial}{\partial y}\left[\mu\left(1 + \frac{\epsilon}{\mu}\right)\frac{\partial u}{\partial y}\right] \tag{2}$$

For conservation of energy:

$$\rho u \frac{\partial H}{\partial x} + \rho v \frac{\partial H}{\partial y} = \frac{\partial}{\partial y}\left\{\frac{\mu}{N_{Pr}}\left[\left(1 + \frac{\epsilon}{\mu}\frac{N_{Pr}}{N_{Pr,t}}\right)\frac{\partial H}{\partial y} - \left(1 - N_{Pr} + \frac{\epsilon}{\mu} N_{Pr} \frac{1 - N_{Pr,t}}{N_{Pr,t}}\right) u \frac{\partial u}{\partial y}\right]\right\} \tag{3}$$

The assumption is made that the eddy viscosity can be represented by the simple Prandtl mixing-length concept across the entire boundary layer. A Van Driest modification (ref. 11) is used near the wall, gas properties being evaluated at wall conditions. The expression for ϵ is thus

$$\epsilon = \rho l^2 \left[1 - \exp\left(\frac{y}{A}\right)\right]^2 \left|\frac{\partial u}{\partial y}\right| \tag{4}$$

where

$$A = -26 \frac{\mu_w}{\rho_w}\left(\frac{\rho_w}{\tau_w}\right)^{1/2}$$

The variation of l/δ with y/δ was based on results from reference 12 and was assumed to be invariant with Mach number. The numerical values used in the present work are given in table I. For the calculations shown herein, $N_{Pr,t}$ was taken as 0.9 (ref. 13) and was assumed to be constant.

The method of solution of equations (1), (2), and (3) is similar to that used in reference 14 and is essentially a linearized form of the implicit finite-difference numerical method of reference 15. As in reference 14, a variable step size in the y-direction is used.

Integral Approach

In the integral method the momentum integral equation for axisymmetric flow (eq. (42), ch. 9 of ref. 16) is solved by a variable-step-size fifth-order Runge-Kutta numerical scheme. In order to solve this equation, H^* and C_f variations must be specified. In the outer part of the boundary layer, a temperature-velocity relationship of the form

$$\tilde{\theta} \equiv \frac{T_t - T_w}{T_{t,\infty} - T_w} = \left(\frac{u}{u_e}\right)^{\alpha} \tag{5}$$

is assumed where the value of α depends on the flow configuration for which calculations are being made. Further discussion of the values assigned to α is given in a subsequent section. Near the wall the total-temperature—velocity relation is obtained from the Colburn form of the Reynolds analogy. The wall total-temperature—velocity relationship is joined to equation (5) by an intermediate linear relationship which matches the wall equation at $\frac{u}{u_e} = 0.01$ and equation (5) at $\frac{u}{u_e} = 0.10$.

The velocity profiles were assumed to be

$$\frac{u}{u_e} = \left(\frac{y}{\delta}\right)^{1/N} \tag{6}$$

where N is a specified function of $R_{e,\theta}$ and T_w/T_t. For calculations of the nozzle-wall boundary layers, this function was taken as the solid line through the data shown in figure 1. The data shown are taken from references 4, 18 to 22. The wall-temperature factor used in the correlation is based on flat-plate type of data at the same Mach number and $R_{e,\theta}$ values but at different T_w/T_t values. Since the present objective is the calculation of air and nitrogen axisymmetric nozzle-wall boundary layers, the data used to define an N variation are limited to these conditions. For those cases where only pitot data were available (shown flagged), the velocity profiles were obtained by using a value of 2 for α in equation (5). (See next section.) The velocity and temperature distributions just described (eqs. (5) and (6)) were used to obtain H^*.

The skin-friction-coefficient expression of Spalding and Chi (ref. 17) was used directly, without any attempt to account for the effects of pressure gradient.

RESULTS AND DISCUSSION

Dependence of Temperature-Velocity Relation on Flow History

As mentioned in the Introduction, the relation between total temperature and velocity may be different for flat-plate and nozzle-wall boundary layers. (See refs. 6, 7, and 8.) A possible cause of this difference is the favorable pressure-gradient history of the nozzle flows. In order to investigate this difference further, all available data where heat transfer was present and the pressure gradient small locally, are shown plotted in figures 2 and 3 in the usual "Crocco" variables $\left(\bar{\theta} \text{ and } \frac{u}{u_e}\right)$. In figure 2 are shown the data which have been obtained on the flat-plate type of configurations, that is, flat plates, hollow cylinders, and in flows where the upstream pressure gradient was small (refs. 24 to 32). Included are unpublished measurements obtained on a flat plate at Mach 6.5 by Hopkins and Keener of NASA Ames Research Center. The amount of scatter exhibited by the data is appreciable, and this scatter may be due to the difficulty of obtaining accurate measurements in the relatively thin boundary layers usually present in this class of configuration. Also, "flat-plate-flow" experiments do not always achieve the uniform conditions implied in the name. Effects due to induced pressures, wall-temperature variations, secondary flows, and proximity of the measuring station to transition may contribute to the scatter in the available data. However, the mean of the data is perhaps adequately represented for engineering purposes by the linear relation shown. As is well known, this linear variation is a solution to the governing differential equations for the special case of zero pressure gradient and turbulent Prandtl number equal to 1. Since the turbulent Prandtl number is probably of the order of 1 (ref. 13, for example), the "agreement" between the flat-plate data and the linear relationship seems to be reasonable.

Shown in figure 3 are the available data (refs. 8, 20 to 22, and 33 to 37) from the "nozzle wall" class of configuration, that is, data obtained on wind-tunnel walls or flat plates and cones where a nozzle type of upstream pressure history was imposed. Included in this figure are the results of the present Mach 8 and 19 measurements. It is apparent that, in contrast to the data in figure 2, the nozzle data are better represented by a quadratic type of relationship ($\alpha = 2$). R. K. Matthews of Arnold Engineering Development Center indicated that unpublished nozzle wall data at Mach 6, 8, and 10 from Arnold Engineering Development Center are also in general agreement with this quadratic trend, as are the data from reference 23.

An indication of possible effects of the upstream pressure gradient history that might account for the apparent difference between the nozzle-wall and flat-plate temperature-velocity relation can be obtained from the present finite-difference calculation method. Calculations were made for the boundary-layer development down the contour of the nozzle from which the Mach 8 data were obtained. The calculation was initiated at the nozzle throat and carried through to the nozzle exit. The variation down the nozzle of the parameters needed for the calculation is shown in figure 4.

Computed total temperature and velocity profiles are shown plotted in figures 5 and 6 for several positions along the nozzle. The input profiles for both u/u_e and $\bar{\theta}$ at the throat were assumed to be 1/7-power-law profiles, that is, the input total-temperature—velocity relation was linear. These profiles are indicated in figures 5 and 6. Downstream of the throat in the favorable pressure-gradient region at $x \approx 5$ inches (12.7 cm) (station 2) the velocity profile has bulged outward, but the total-temperature profile has actually become less full. As can be seen from figure 6, these results lead to a temperature-velocity variation similar to that measured further downstream on the nozzle walls. (See fig. 3.) At the measuring station near the nozzle exit, where the pressure gradient is locally small, the velocity profile is still considerably fuller than the total-temperature profile. This condition perhaps indicates that the boundary layer has not yet relaxed to an equilibrium state. Profiles computed downstream indicate that the temperature-velocity relation tends to approach the linear variation with increasing downstream distance. (Further calculations have indicated that the predicted temperature-velocity relation at the nozzle exit is not a strong function of the input profiles at the throat.)

There is another mechanism present in at least some of the available nozzle-wall investigations which could produce a decrease in the total temperature in the wall boundary layer. In the Mach 6 measurements reported herein, it was found that there was a layer of air adjacent to the settling chamber liner which was much cooler than the rest of the flow. If this thermal layer expands down the nozzle without mixing, the nozzle-wall boundary layer would be growing in a cooler effective free stream until the cool-layer mass flow is absorbed or swallowed in the wall boundary. Estimates of this "swallowing" distance give values of up to half the nozzle length for some cases, and it is possible that the effect within the boundary layer of the cooled mass could persist downstream much farther.

The previous discussion has indicated that turbulent boundary layers on nozzle walls at positions where measurements are usually made may not be in equilibrium in the sense that the effects of upstream pressure gradients and/or thermal layers can persist for large downstream distances. However, the nozzle data are useful for at least two purposes: (1) The data can be used to improve prediction methods for boundary-layer displacement effects in hypersonic nozzle design; and (2) these data can provide valuable test cases for the development of nonsimilar finite-difference methods. That is, the numerical solutions for nozzle flows can be used to evaluate the range of conditions for which models of the turbulent shear term (usually based on equilibrium data) are applicable.

Application of Theories to Mach 6, 8, and 19 Nozzle-Wall Data

Mach 8 measurements at nozzle exit.- Pitot-pressure and total-temperature measurements have been obtained by William V. Feller and Robert A. Jones of Langley Research Center in the wall boundary layer at the nozzle exit of the Langley Mach 8 variable-density wind tunnel which is described briefly in reference 38. These data in the form of velocity and Mach number profiles and plots of $\bar{\theta}$ against u/u_e are shown in figures 7, 8, and 9. Predictions from the integral and finite-difference methods are also indicated. (A tabulation of the faired experimental profiles is given in table II.)

The measured and theoretical velocity distributions are plotted in figure 7 as a function of y, the physical distance from the wall. Both methods predict the velocity profile data with acceptable engineering accuracy. As can be seen in the table included in the figure, both theories give a fair prediction of the integral parameters θ and δ^*.

The corresponding experimental Mach number profile shown in figure 8 is predicted accurately by the integral theory over most of the boundary layer. The finite-difference theory underpredicts the Mach number through most of the boundary layer and indicates that the theoretical total-temperature profile is too full since the velocity prediction was correct. The total-temperature—velocity plots for the Reynolds number range of the tests are shown in figure 9. All the data are more or less in agreement with the quadratic type of temperature-velocity relationship. Also, within the data scatter there seems to be little effect of Reynolds number. The finite-difference theory predicts too rapid a recovery toward the linear variation (or a final total-temperature profile that is too full). This result is reasonable since the eddy viscosity model used (eq. (4)) is based on equilibrium data and hence might be expected to drive the flow toward equilibrium too rapidly. (Further evaluation of the present eddy viscosity model is presented in ref. 39.) However, the additional mechanism referred to previously (enthalpy deficit in settling chamber flow) could cause reduced total temperatures within the boundary layer and hence might be partly responsible for the disagreement between theory and data.

Mach 19 measurements at nozzle exit.- Pitot-pressure and total-temperature measurements at Mach 19 have been obtained by William D. Harvey and Frank L. Clark of Langley Research Center in the wall boundary layer at the nozzle exit of the hypersonic nitrogen facility at the Langley Research Center which is described in reference 40. Velocity and Mach number profiles and total temperature-velocity plots obtained from these data are shown in figures 10, 11, and 12 along with the predictions of the integral method. (A tabulation of the faired experimental profiles is given in table III.)

In the outer section of the velocity profile shown in figure 10, the prediction of the integral theory agrees with the measurements. However, in the inner region the prediction deviates from the data considerably. This discrepancy is due to the fact that a power-law representation of the profile is not valid in the viscous sublayer which, for the present conditions, extends out to values of y that are from 20 to 40 percent of the boundary-layer thickness. The accuracy of the present integral method is therefore limited by the assumption of a power-law velocity profile. The prediction of the integral theory for the Mach number profile shown in figure 11 is not very satisfactory. The reason for disagreement in the inner region of the boundary layer is probably the overprediction of the velocity as seen in figure 10. The variation of total temperature with velocity indicated by the data is shown in figure 12. The data are seen to be above the quadratic variation.

Mach 6 measurements at and downstream of nozzle exit.- Pitot-pressure and total-temperature measurements have been obtained by William V. Feller and Robert A. Jones of Langley Research Center in the boundary layer of the Langley Mach 6 high Reynolds number tunnel both at the nozzle exit and at several stations along a straight-pipe extension downstream of the nozzle exit. This facility has recently become operational and has a contoured axisymmetric nozzle with a 6° maximum turning angle and a nominal test-section diameter of 12 inches (30.48 cm). Velocity and Mach number profiles at the nozzle exit are shown in figures 13 and 14, whereas the temperature-velocity data for the various stations along the straight extension are shown in figure 15.

The velocity profile data shown in figure 13 are in good agreement with the integral-theory prediction, as are the integral parameters θ and δ^*. (See table in fig. 13.) The predicted Mach number profile shown in figure 14 is also in reasonable agreement with the data.

The variations of total temperature with velocity are shown in figure 15 for various positions along the straight-pipe extension. The data at the first three measuring stations (94 in. (238.7 cm), 124 in. (315 cm), and 172 in. (436.7 cm) downstream of the throat) are seen to be nearly the same and are in general agreement with quadratic variation. However, the data at the last measuring station, which is some 60 boundary-layer thicknesses (using an average δ of 2 in. (5.08 cm)) downstream of the nozzle exit, show a tendency towards the linear variation. In an unpublished U.S. Naval Ordnance Laboratory investigation by Lee and Yanta at some 30 boundary-layer thicknesses downstream of their nozzle exit (start of $dp/dx \approx 0$ flow along straight section), they were unable to detect any tendency toward a linear variation. Thus large distances may be necessary in nozzle flows before recovery toward a linear temperature-velocity variation occurs.

CONCLUDING REMARKS

Comparison of available flat-plate and nozzle-wall turbulent-boundary-layer data indicates that the variation of total temperature with velocity is generally different in the two types of flow. Data for the flat-plate flows show considerable scatter but the average exhibits a linear type of relationship as opposed to the more quadratic variation always found in the nozzle data. Results of nonsimilar finite-difference calculations for the nozzle flows indicate that at least part of this difference is caused by the favorable pressure-gradient history.

Profile measurements along a straight section downstream of the nozzle exit of a Mach 6 tunnel indicate that a distance on the order of 60 boundary-layer thicknesses may be necessary before the flow begins to revert (or relax) toward a linear temperature-velocity variation which is perhaps typical of flat-plate type of flows.

The simple integral method used herein includes correlations taken from nozzle wall data and gives results in good agreement with nozzle profile measurements at Mach 6 and 8 and in reasonable agreement at Mach 18.

Langley Research Center,
National Aeronautics and Space Administration,
Langley Station, Hampton, Va., July 18, 1969.

REFERENCES

1. Sterrett, James R.; Morrisette, E. Leon; Whitehead, Allen H., Jr.; and Hicks, Raymond M.: Transition Fixing for Hypersonic Flow. NASA TN D-4129, 1967.

2. Sivells, James C.; and Payne, Robert G.: A Method of Calculating Turbulent-Boundary-Layer Growth at Hypersonic Mach Numbers. AEDC-TR-59-3, DDC Doc. No. AD208774, Arnold Eng. Dev. Center, Mar. 1959.

3. Persh, Jerome; and Lee, Roland: A Method for Calculating Turbulent Boundary Layer Development in Supersonic and Hypersonic Nozzles Including the Effects of Heat Transfer. NAVORD Rep. 4200 (Aeroballistic Res. Rep. 320), U.S. Naval Ord. Lab. (White Oak, Md.), June 7, 1956.

4. Michel, R.: Developpement de la Couche Limite Dans Une Tuyere Hypersonique. The High Temperature Aspects of Hypersonic Flow, Wilbur C. Nelson, ed., Pergamon Press, c.1964, pp. 693-716.

5. Wallace, J. E.: Hypersonic Turbulent Boundary-Layer Studies at Cold Wall Conditions. Proceedings of the 1967 Heat Transfer and Fluid Mechanics Institute, Paul A. Libby, Daniel B. Olfe, Charles W. Van Atta, eds., Standford Univ. Press, c.1967, pp. 427-451.

6. Seiff, Alvin; and Short, Barbara J.: An Investigation of Supersonic Turbulent Boundary Layers on Slender Bodies of Revolution in Free Flight by Use of a Mach-Zehnder Interferometer and Shadowgraphs. NACA TN 4364, 1958.

7. Rotta, J. C.: Recent Developments in Calculation Methods for Turbulent Boundary Layers With Pressure Gradients and Heat Transfer. Trans. ASME, J. Appl. Mech., vol. 33, ser. E., no. 2, June 1966, pp. 429-437.

8. Bertram, Mitchel H.; and Neal, Luther, Jr.: Recent Experiments in Hypersonic Turbulent Boundary Layers. Presented to the AGARD Specialists Meeting on Recent Developments in Boundary-Layer Research (Naples, Italy), May 10-14, 1965.

9. Smith, A. M. O.; and Cebeci, T.: Numerical Solution of the Turbulent-Boundary-Layer Equations. Report No. DAC 33735 (Contract NOw 66-0324-C), Douglas Aircraft Co., Inc., May 29, 1967.

10. Schubauer, Galen B.; and Tchen, C. M.: Free Turbulent Flows. Turbulent Flows and Heat Transfer. Vol. V of High Speed Aerodynamics and Jet Propulsion, C. C. Lin, ed., Princeton Univ. Press, 1959, pp. 158-184.

11. Van Driest, E. R.: On Turbulent Flow Near a Wall. J. Aeron. Sci., vol. 23, no. 11, Nov. 1956, pp. 1007-1011.

12. Maise, George; and McDonald, Henry: Mixing Length and Kinematic Eddy Viscosity in a Compressible Boundary Layer. AIAA J., vol. 6, no. 1, Jan. 1968, pp. 73-80.

13. Morkovin, Mark V.: Effects of Compressibility on Turbulent Flows. The Mechanics of Turbulence, Gordon and Breach Science Publ., c.1964, pp. 367-380.

14. Beckwith, Ivan E.; and Bushnell, Dennis M. (With appendix C by Carolyn C. Thomas): Detailed Description and Results of a Method for Computing Mean and Fluctuating Quantities in Turbulent Boundary Layers. NASA TN D-4815, 1968.

15. Blottner, F. G.: Nonequilibrium Laminar Boundary-Layer Flow of Ionized Air. AIAA J., vol. 2, no. 11, Nov. 1964, pp. 1921-1927.

16. Fluid Motion Sub-Committee of the Aeronautical Research Council: Modern Developments in Fluid Dynamics. High Speed Flow. Vol. I, L. Howarth, ed., Clarendon Press (Oxford), 1953.

17. Spalding, D. B.; and Chi, S. W.: The Drag of a Compressible Turbulent Boundary Layer on a Smooth Flat Plate With and Without Heat Transfer. J. Fluid Mech., vol. 18, pt. 1, Jan. 1964, pp. 117-143.

18. Persh, Jerome: A Theoretical Investigation of Turbulent Boundary Layer Flow With Heat Transfer at Supersonic and Hypersonic Speeds. NAVORD Rep. 3854, U.S. Naval Ord. Lab. (White Oak, Md.), May 19, 1955.

19. Burke, Andrew F.: Turbulent Boundary Layers on Highly Cooled Surfaces at High Mach Numbers. Proceedings of Symposium on Aerothermoelasticity, ASD Tech. Rep. 61-645, U.S. Air Force, 1961, pp. 704-741.

20. Hill, F. K.: Appendix II – Skin Friction and Heat Transfer Measurements at Mach Numbers From 8-10 in Turbulent Boundary Layers. Bumblebee Aerodynamics Panel. TG-14-37, vol. I, Appl. Phys. Lab., John Hopkins Univ., May 1959, pp. 15-26.

21. Perry, J. H.; and East, R. A.: Experimental Measurements of Cold Wall Turbulent Hypersonic Boundary Layers. AGARD CP No. 30, May 1968, pp. 2-1 – 2-19.

22. Scaggs, Norman E.: Boundary Layer Profile Measurements in Hypersonic Nozzles. ARL 66-0141, U.S. Air Force, July 1966.

23. Shall, Paul Joseph, Jr.: A Boundary Layer Study on Hypersonic Nozzles. M.S. Thesis, U.S. Air Force Institute of Technology, Mar. 1968. (Available from DDC as AD 833236.)

24. Winkler, Eva M.; and Cha, Moon H.: Investigation of Flat Plate Hypersonic Turbulent Boundary Layers With Heat Transfer at a Mach Number of 5.2. NAVORD Rep. 6631, U.S. Nav. Ord. Lab., Sept. 15, 1959.

25. Danberg, James E.: Characteristics of the Turbulent Boundary Layer With Heat and Mass Transfer: Data Tabulation. NOLTR 67-6, U.S. Naval Ordnance Laboratory (White Oak, Md.), Jan. 23, 1967. (Available from DDC as AD 650272.)

26. Samuels, Richard D.; Peterson, John B., Jr.; and Adcock, Jerry B.: Experimental Investigation of the Turbulent Boundary Layer at a Mach Number of 6 With Heat Transfer at High Reynolds Numbers. NASA TN D-3858, 1967.

27. Danberg, James E.: Measurement of the Characteristics of the Compressible Turbulent Boundary Layer With Air Injection. NAVORD Report 6683, U.S. Nav. Ord. Lab., Sept. 3, 1959.

28. Softley, Eric J.; and Sullivan, Robert J.: Theory and Experiment for the Structure of Some Hypersonic Boundary Layers. AGARD CP No. 30, May 1968, pp. 3-1 – 3-18.

29. Swanson, Andrew G.; Buglia, James J.; and Chauvin, Leo T.: Flight Measurements of Boundary-Layer Temperature Profiles on a Body of Revolution (NACA RM-10) at Mach Numbers From 1.2 to 3.5. NACA TN 4061, 1957.

30. Hoydysh, Walter G.; and Zakkay, Victor: An Experimental Investigation of Hypersonic Turbulent Boundary Layers in Adverse Pressure Gradient. AIAA J., vol. 7, no. 1, Jan. 1969, pp. 105-116.

31. Watson, E. C.; Gnos, A. V.; Gallo, W. F.; and Latham, E. A.: Boundary Layers and Hypersonic Inlet Flow Fields. AIAA Paper No. 66-606, June 1966.

32. Stroud, J. F.; and Miller, L. D.: An Experimental and Analytical Investigation of Hypersonic Inlet Boundary Layers. Volume II. Data Reduction Program and Tabulated Experimental Data. AFFDL-TR-65-123 – Vol. II, U.S. Air Force, Aug. 1965. (Available from DDC as AD 621344.)

33. Lobb, R. Kenneth; Winkler, Eva M.; and Persh, Jerome: Experimental Investigation of Turbulent Boundary Layers in Hypersonic Flow. J. Aeronaut. Sci., vol. 22, no. 1, Jan. 1955, pp. 1-9,50.

34. Lee, Roland E.; Yanta, William J.; and Leonas, Annette C.: Velocity Profile, Skin Friction Balance and Heat Transfer Measurements of the Turbulent Boundary Layer at Mach 5. Proceedings of the 1968 Heat Transfer and Fluid Mechanics Institute, Ashley F. Emery and Creighton A. Depew, eds., Stanford Univ. Press, c.1968.

35. Pasiuk, Lionel; Hastings, Samuel M.; and Chatham, Rodney: Experimental Reynolds Analogy Factor for a Compressible Turbulent Boundary Layer With a Pressure Gradient. NOL TR 64-200, U.S. Naval Ordnance Lab. (White Oak, Md.), Nov. 27, 1964.

36. Sheer, R. E., Jr.; and Nagamatsu, H. T.: Methods for Distinguishing Type of Hypersonic Boundary Layer in Shock Tunnel. AIAA Paper No. 68-50, Jan. 1968.

37. Wallace, J. E.: Hypersonic Turbulent Boundary Layer Measurements Using an Electron Beam. CAL Rep. No. AN-2112-Y-1, Cornell Aeronaut. Lab., Inc., Aug. 1968.

38. Schaefer, William T., Jr.: Characteristics of Major Active Wind Tunnels at the Langley Research Center. NASA TM X-1130, 1965.

39. Bushnell, D. M.; and Beckwith, I. E.: Calculation of Nonequilibrium Hypersonic Turbulent Boundary Layers and Comparisons With Experimental Data. AIAA Preprint No. 69-684, 1969.

40. Clark, Frank L.; Ellison, James C.; and Johnson, Charles B.: Recent Work in Flow Evaluation and Techniques of Operations for the Langley Hypersonic Nitrogen Facility. NASA paper presented at Fifth Hypervelocity Techniques Symposium (Denver, Colo.), Mar. 28-30, 1967.

TABLE I.- MIXING LENGTH VARIATION USED IN FINITE-DIFFERENCE THEORY

y/δ	l/δ
0	0
.05	.02
.1	.04
.15	.055
.2	.063
.25	.0725
.3	.08
.35	.083
.4	.0875
.45	.09
.5	.09
.55	.09
.6	.09
.65	.09
.7	.09
.75	.09
.8	.09
.85	.09
.9	.09
.95	.09
1.0	.09
1.4	.09

TABLE II.- DETAILS OF MACH 8 PROFILE

$\left[M_\infty = 7.99, \quad \theta = 0.239\text{ cm}, \quad \delta^* = 2.609\text{ cm}, \quad T_w/T_{t,\infty} = 0.43, \quad R_{e,\theta} = 3.1 \times 10^4\right]$

y, cm	u/u_e	M	$T_t/T_{t,\infty}$
0	0	0	0.43
.254	.67	2.61	.725
.381	.715	2.94	.755
.635	.766	3.36	.791
1.27	.827	4.06	.830
1.90	.864	4.67	.855
2.54	.895	5.26	.881
3.18	.918	5.86	.90
3.81	.935	6.41	.915
4.44	.951	6.90	.932
5.08	.966	7.32	.95
5.72	.980	7.63	.971
6.35	.990	7.80	.986
6.98	.996	7.90	.995
7.62	.999	7.98	.999
8.26	1.0	7.99	1.0

TABLE III.- DETAILS OF MACH 19 PROFILE

[$M_\infty = 19.47$, $\theta = 0.185$ cm, $\delta^* = 4.84$ cm,
$T_w/T_{t,\infty} = 0.177$, $R_{e,\theta} = 5.14 \times 10^3$]

y, cm	u/u_e	M	$T_t/T_{t,\infty}$
0	0	0	0.177
.202	.074	.33	.254
.634	.260	1.25	.281
1.142	.464	2.55	.377
1.650	.586	3.35	.489
2.158	.683	4.40	.579
2.666	.761	5.50	.667
3.174	.810	6.75	.720
3.682	.838	8.00	.748
4.190	.859	9.20	.773
4.698	.881	10.4	.801
5.206	.877	11.60	.789
5.714	.889	12.70	.806
6.222	.928	13.85	.872
6.730	.939	14.95	.890
7.238	.965	16.00	.937
7.746	.974	17.10	.954
8.254	.981	18.85	.964
8.762	.999	19.05	.999
9.270	1.000	19.45	1.000

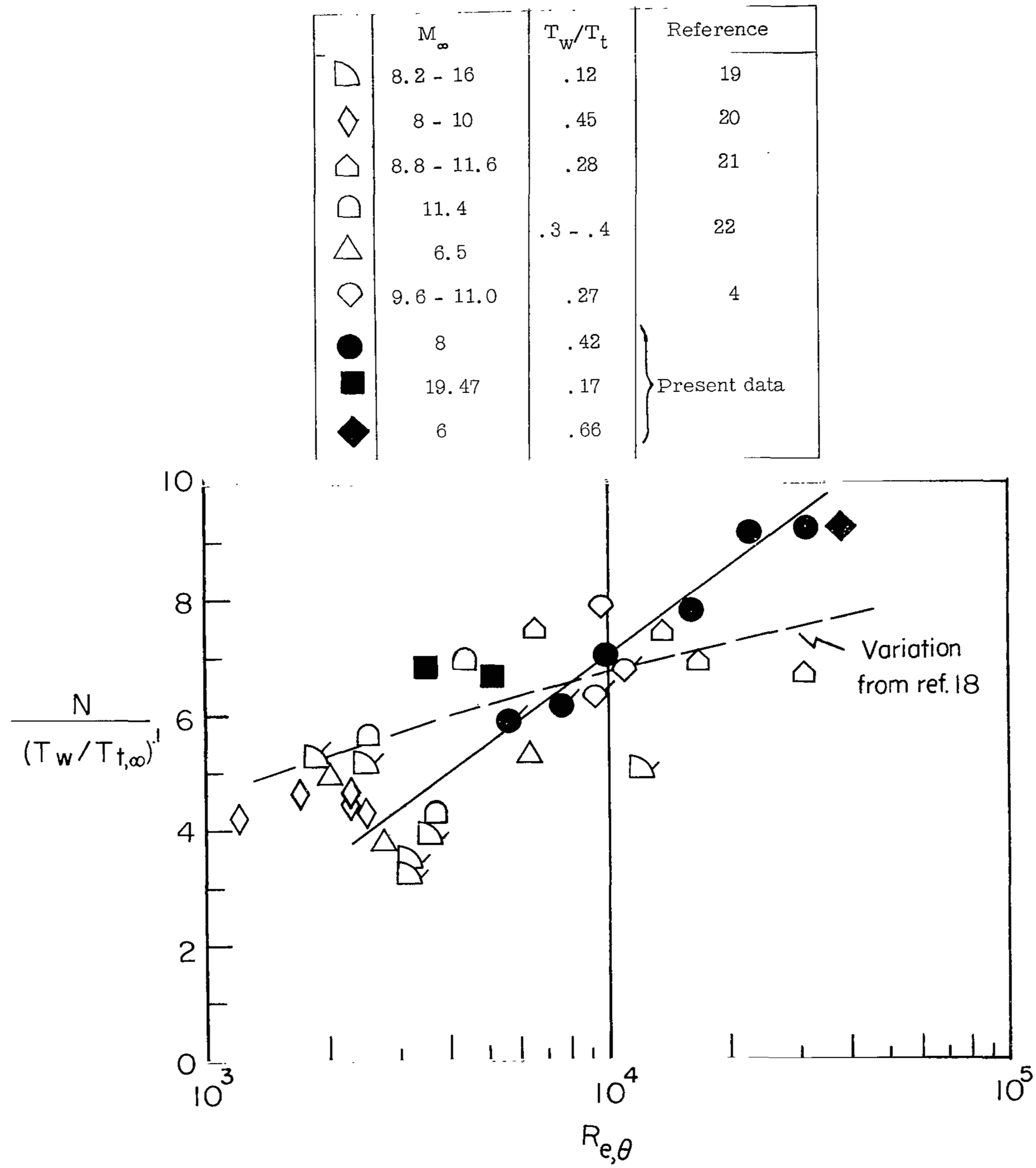

Figure 1.- Variation of N with $R_{e,\theta}$ for axisymmetric air and nitrogen nozzle data. Flagged symbols are data reduced from pitot by using $\alpha = 2.0$. $6 \leq M_\infty \leq 18$; $0.1 \leq \frac{T_w}{T_{t,\infty}} \leq 0.7$.

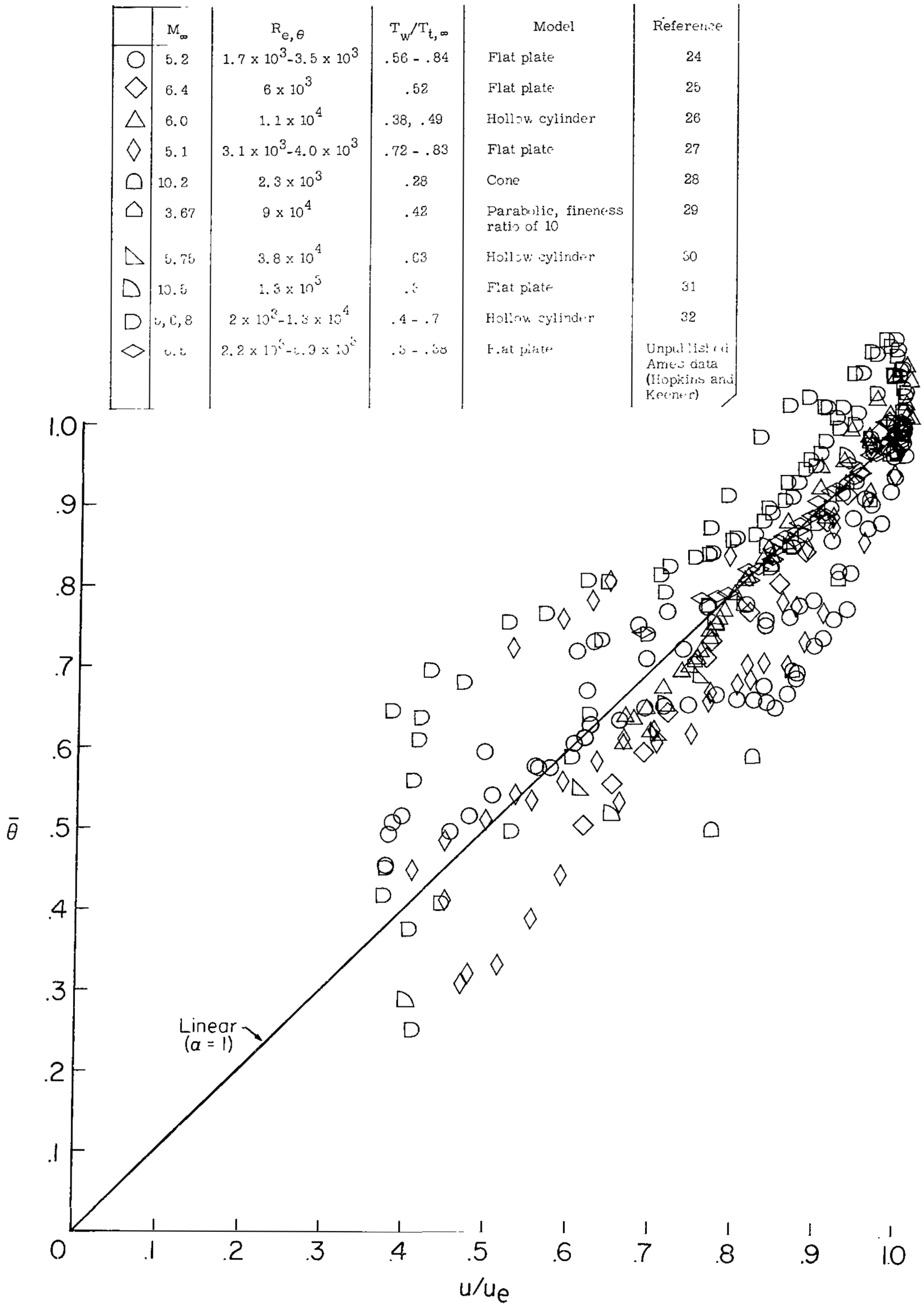

Figure 2.- Total temperature-velocity data for "flat plate" flows. $3.67 \leqq M_\infty \leqq 10.5$; $0.28 \leqq \frac{T_w}{T_{t,\infty}} \leqq 0.84$.

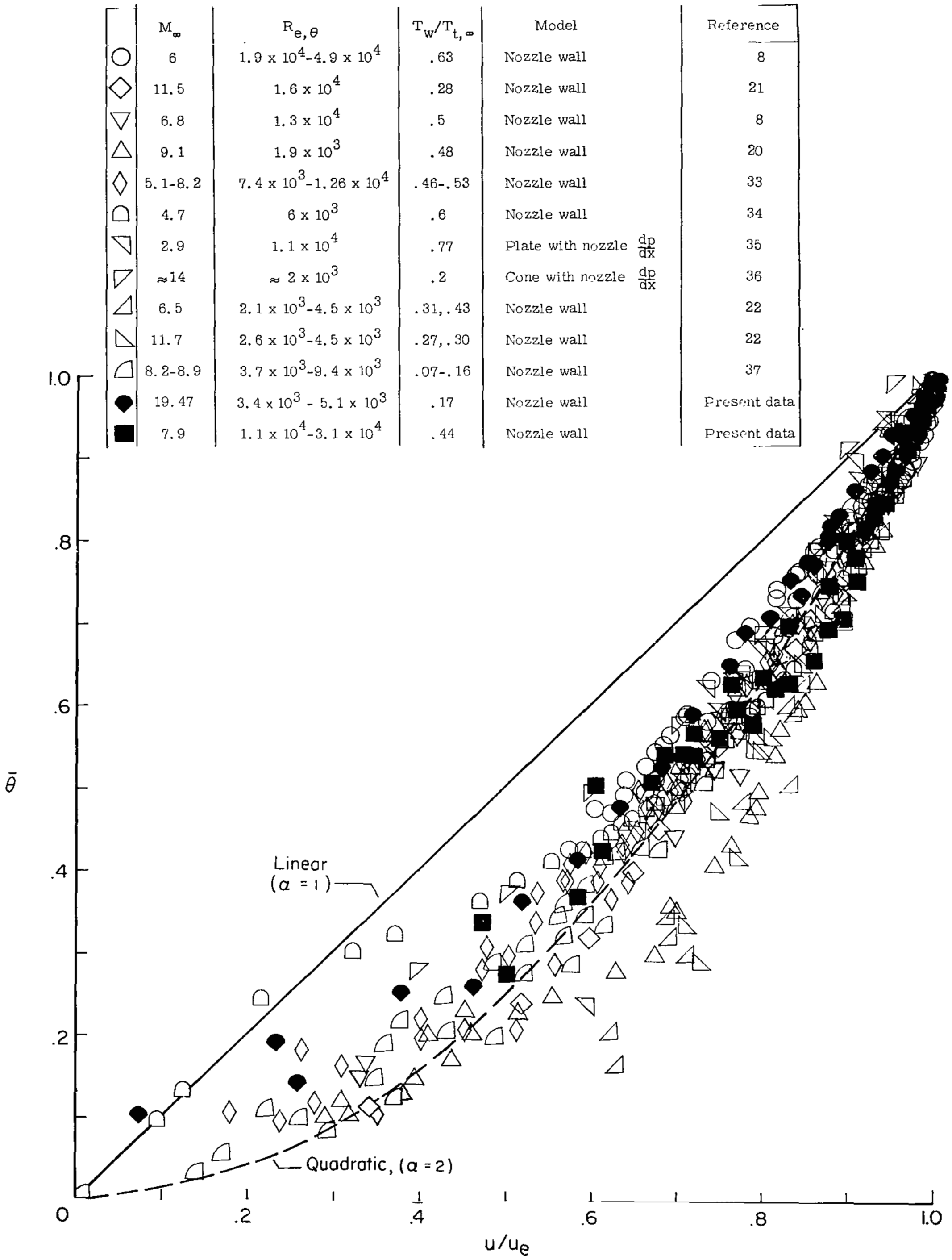

	M_∞	$R_{e,\theta}$	$T_w/T_{t,\infty}$	Model	Reference
○	6	1.9×10^4-4.9×10^4	.63	Nozzle wall	8
◇	11.5	1.6×10^4	.28	Nozzle wall	21
▽	6.8	1.3×10^4	.5	Nozzle wall	8
△	9.1	1.9×10^3	.48	Nozzle wall	20
◊	5.1-8.2	7.4×10^3-1.26×10^4	.46-.53	Nozzle wall	33
⌓	4.7	6×10^3	.6	Nozzle wall	34
◹	2.9	1.1×10^4	.77	Plate with nozzle $\frac{dp}{dx}$	35
◸	≈14	≈ 2×10^3	.2	Cone with nozzle $\frac{dp}{dx}$	36
◿	6.5	2.1×10^3-4.5×10^3	.31, .43	Nozzle wall	22
◺	11.7	2.6×10^3-4.5×10^3	.27, .30	Nozzle wall	22
◿	8.2-8.9	3.7×10^3-9.4×10^3	.07-.16	Nozzle wall	37
●	19.47	3.4×10^3 - 5.1×10^3	.17	Nozzle wall	Present data
■	7.9	1.1×10^4-3.1×10^4	.44	Nozzle wall	Present data

Figure 3.- Total temperature-velocity data for "nozzle wall" flows. $3 \leqq M_\infty \leqq 19$; $0.1 \leqq \frac{T_w}{T_{t,\infty}} \leqq 0.8$.

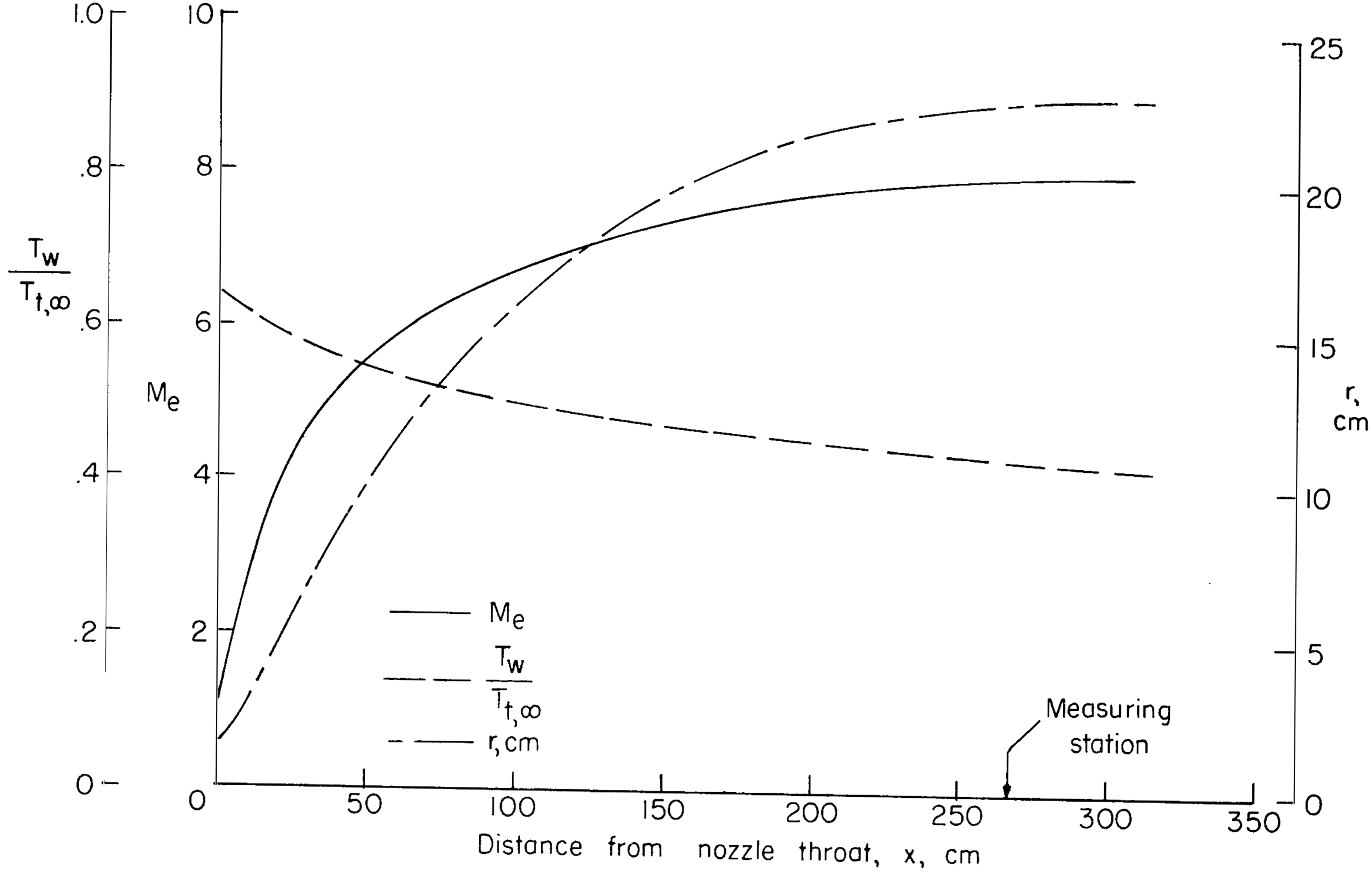

Figure 4.- Parameters for Mach 8 nozzle calculation.

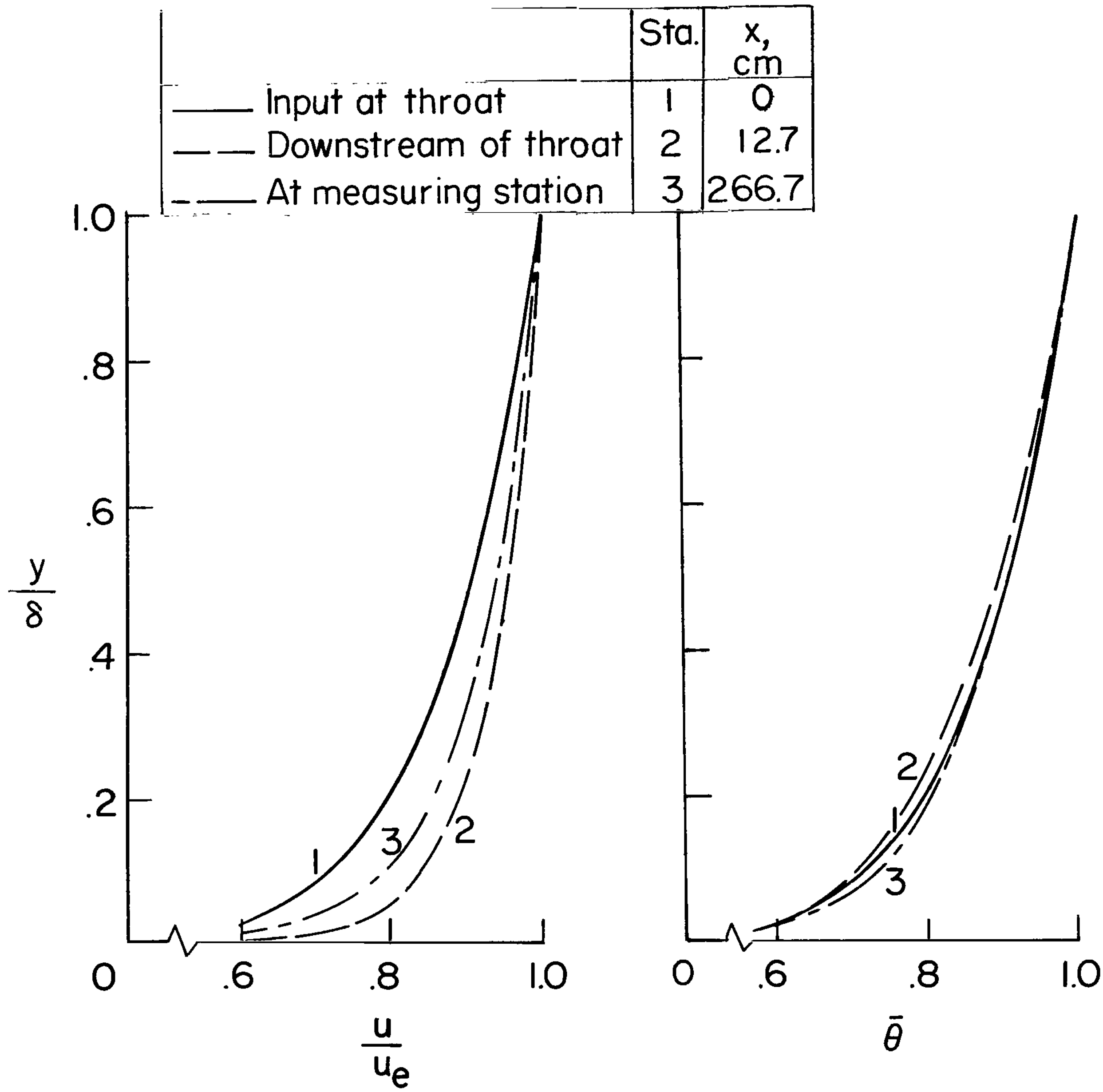

Figure 5.- Velocity and total temperature profiles predicted by finite-difference theory for various positions along Mach 8 nozzle.

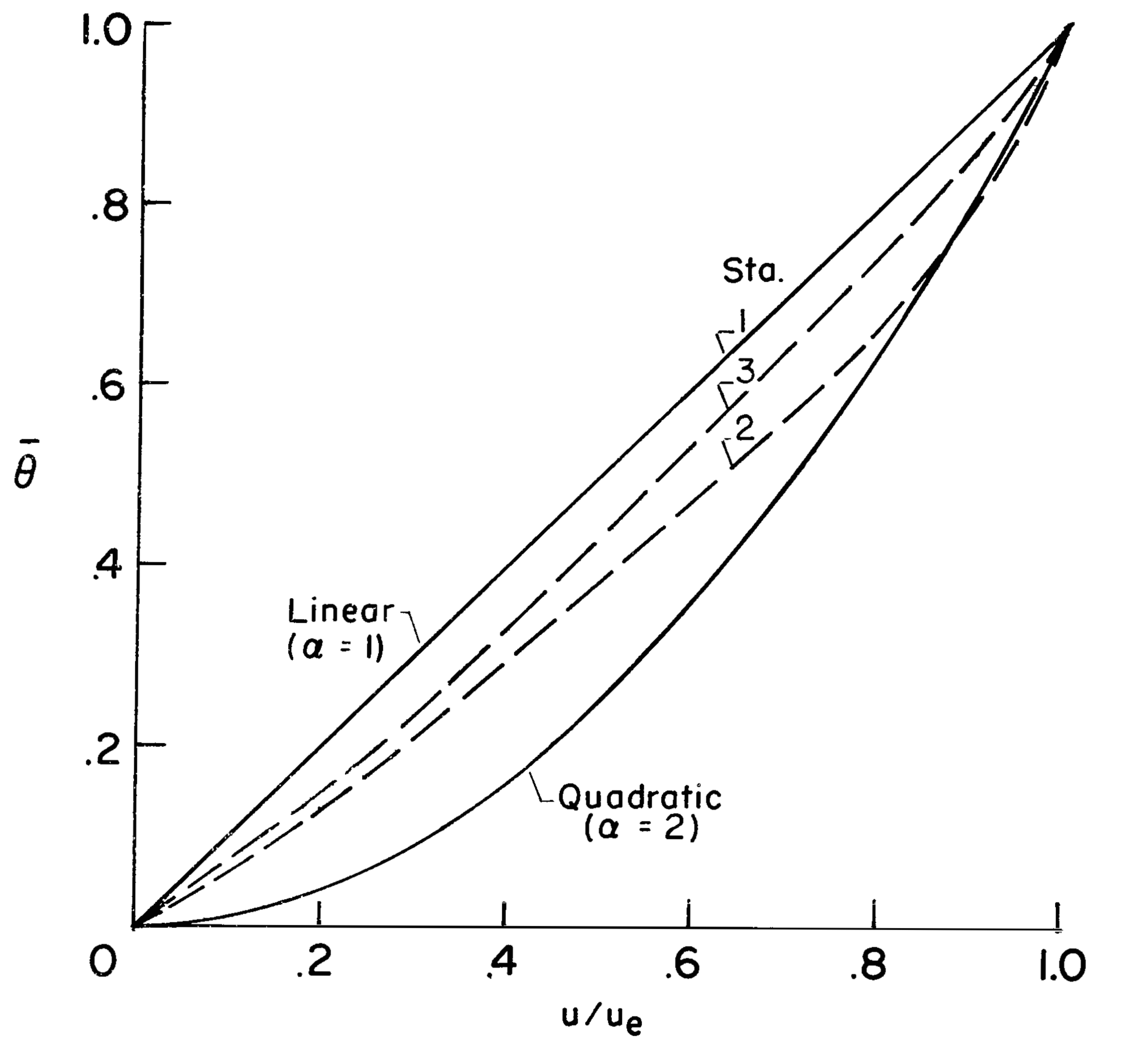

Figure 6.- Predicted total temperature-velocity relationships for Mach 8 nozzle flow from finite-difference theory. Stations are the same as those of figure 5.

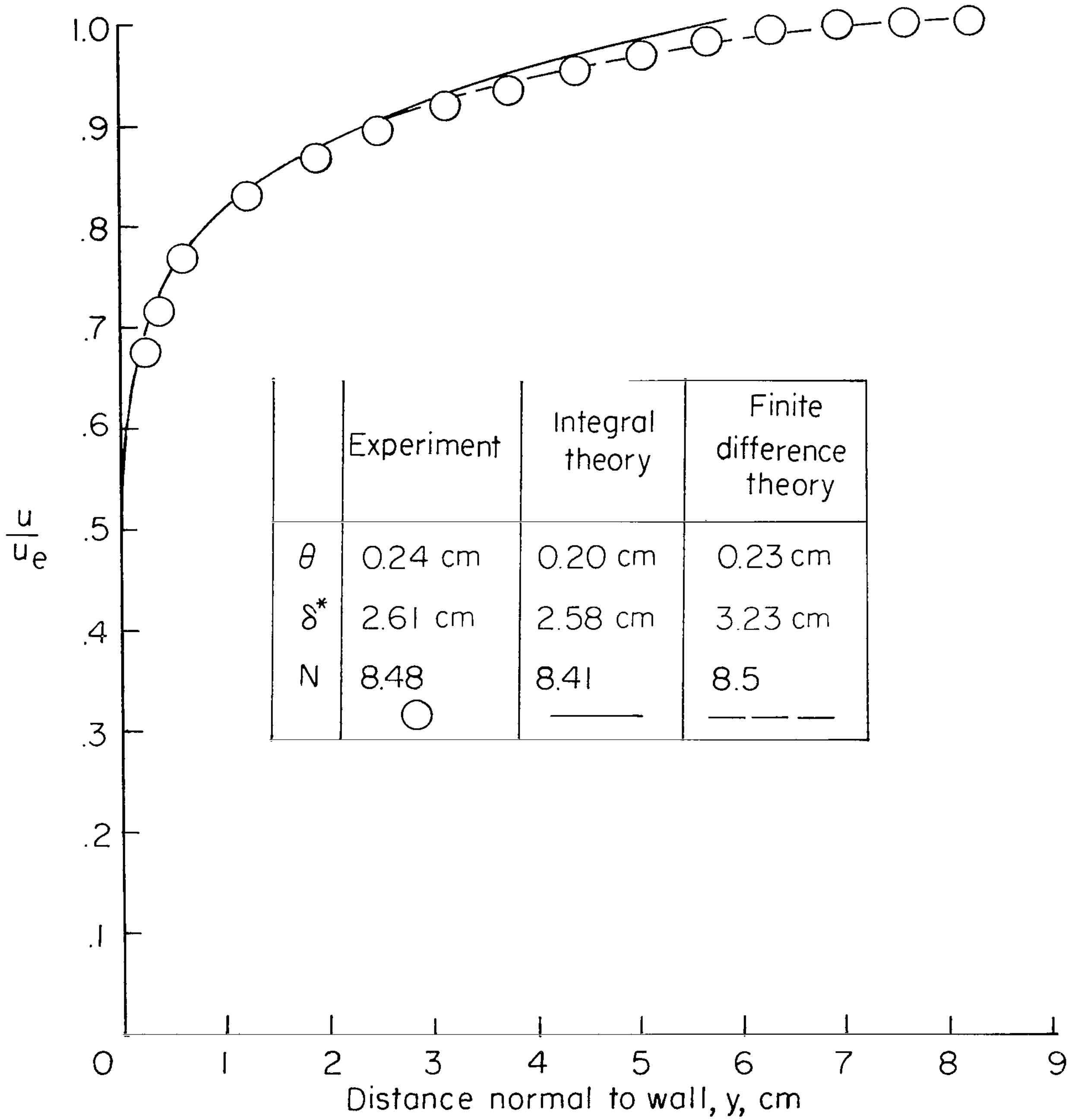

Figure 7.- Turbulent boundary-layer velocity profile at exit of Mach 8 contoured axisymmetric tunnel. $R_{e,\theta} = 3.1 \times 10^4$; $M_\infty = 7.99$; $\frac{T_w}{T_{t,\infty}} = 0.43$.

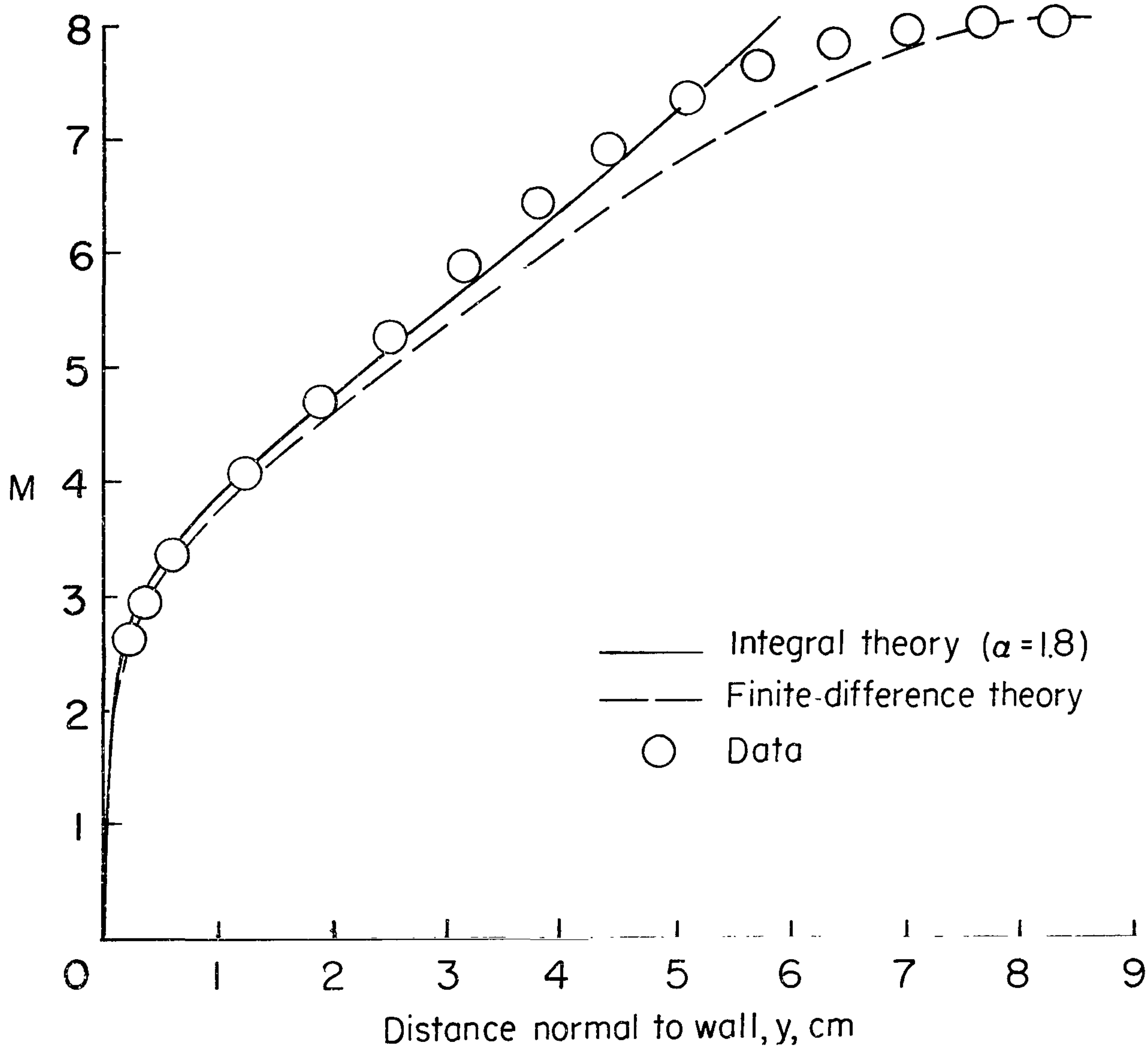

Figure 8.- Mach number profile at exit of Mach 8 nozzle. $R_{e,\theta} = 3.1 \times 10^4$; $M_\infty = 7.99$; $\frac{T_w}{T_{t,\infty}} = 0.43$.

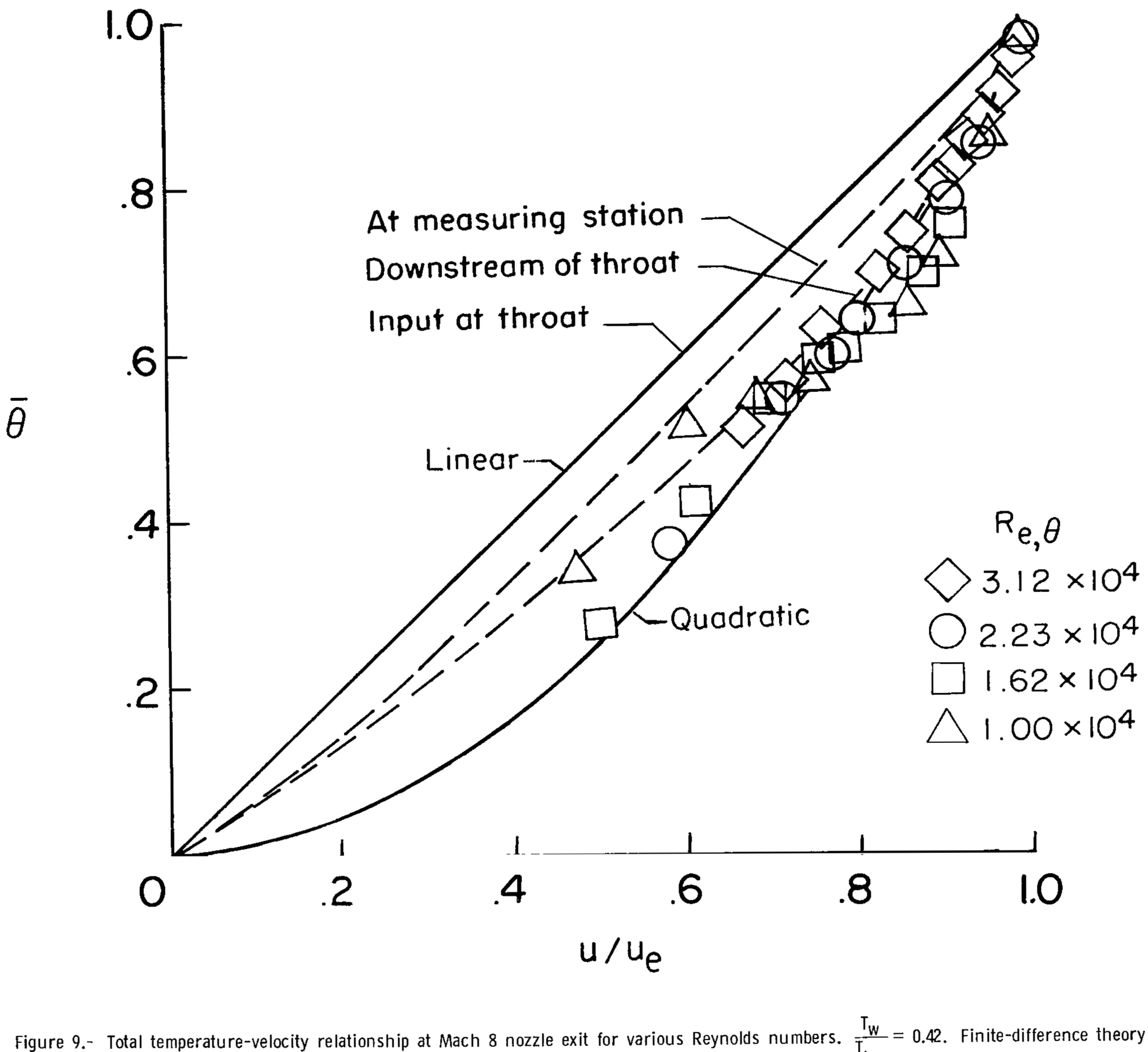

Figure 9.- Total temperature-velocity relationship at Mach 8 nozzle exit for various Reynolds numbers. $\frac{T_w}{T_{t,\infty}} = 0.42$. Finite-difference theory shown for $R_{e,\theta} = 3.12 \times 10^4$ at stations indicated.

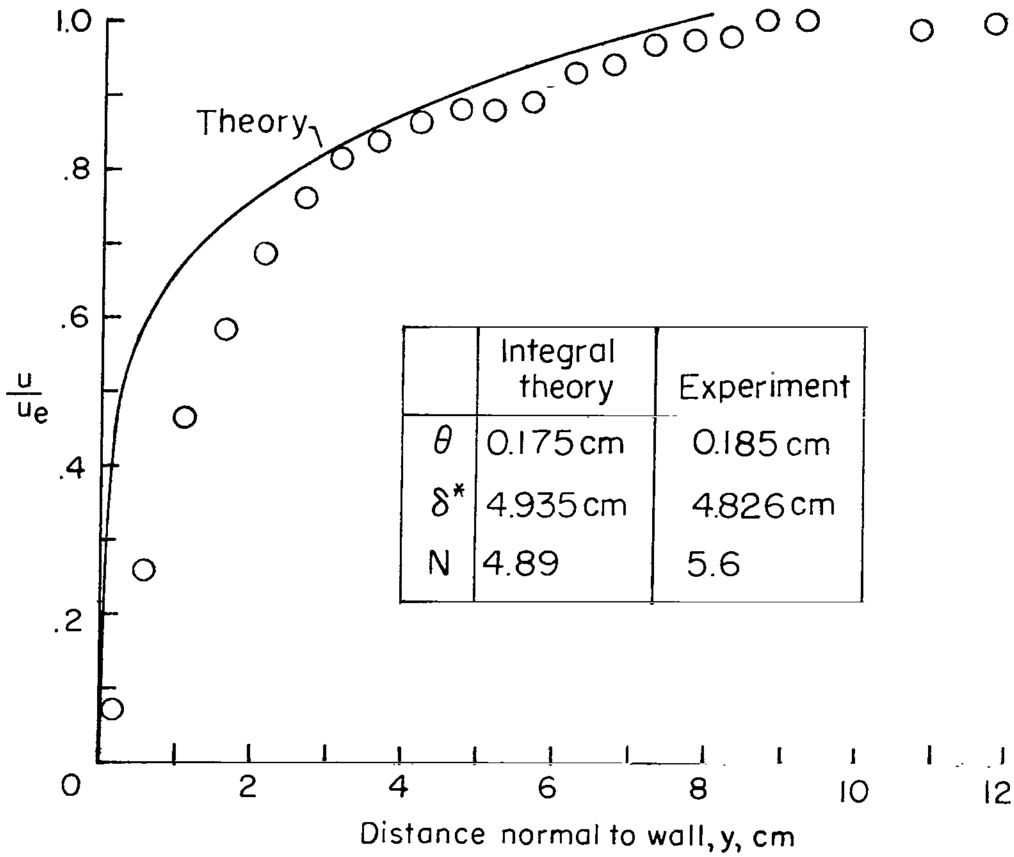

	Integral theory	Experiment
θ	0.175 cm	0.185 cm
δ^*	4.935 cm	4.826 cm
N	4.89	5.6

Figure 10.- Measured turbulent boundary-layer velocity profile at exit of Mach 19 contoured axisymmetric tunnel compared with prediction of integral theory using $\alpha = 2.0$; $R_{e,\theta} = 5.17 \times 10^3$; $\frac{T_w}{T_{t,\infty}} = 0.17$.

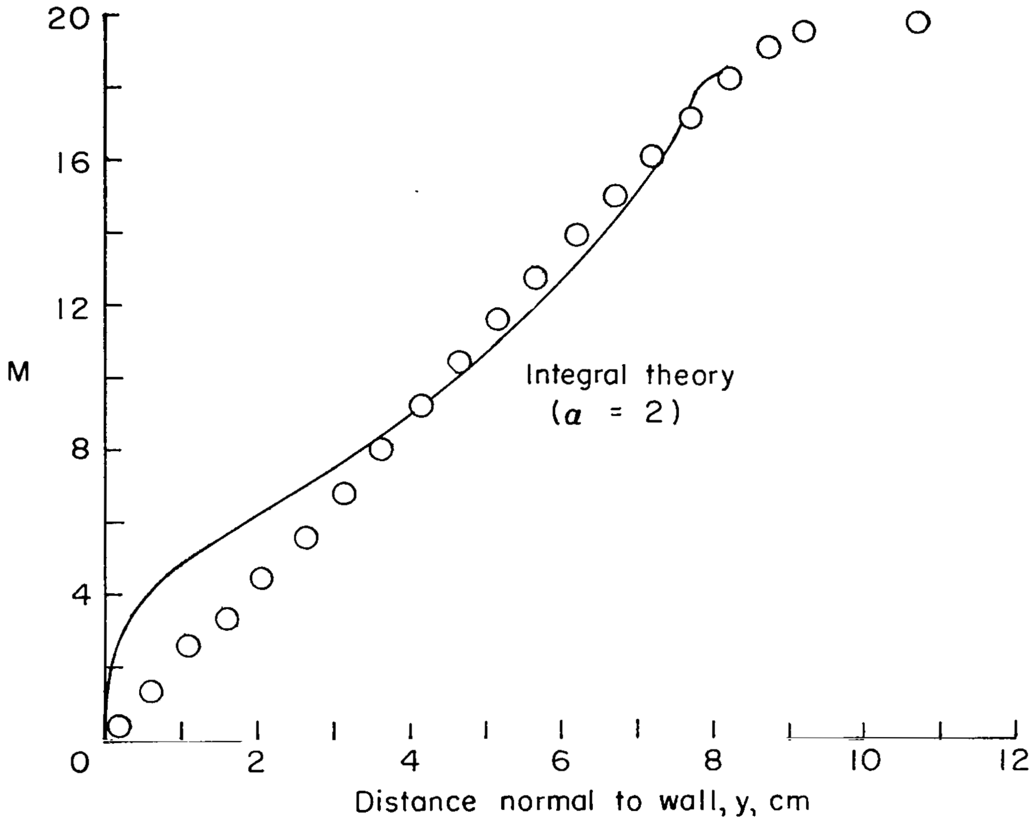

Figure 11.- Mach number profile at exit of Mach 19 nozzle. $R_{e,\theta} = 3.97 \times 10^3$; $\frac{T_w}{T_{t,\infty}} = 0.17$.

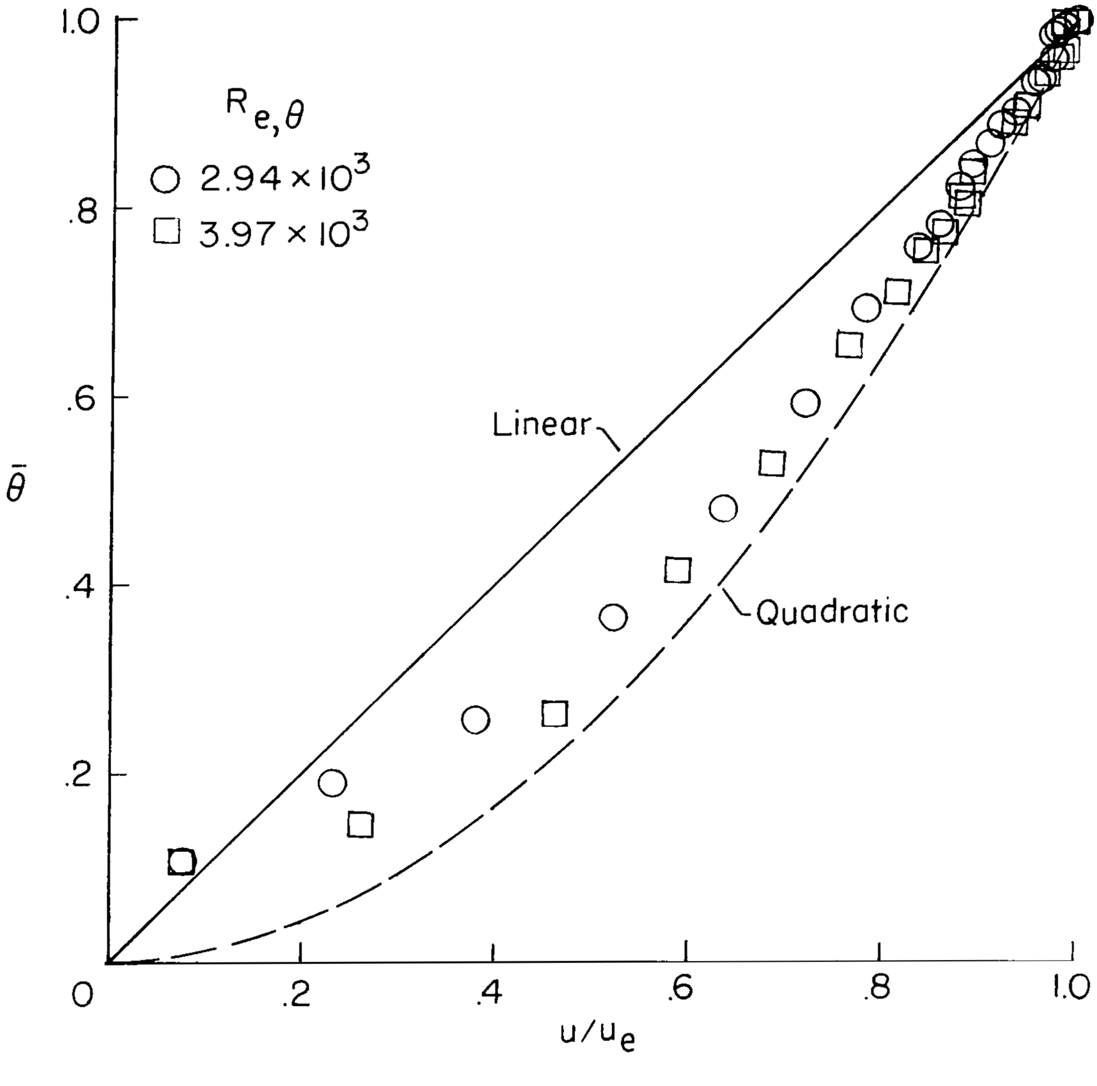

Figure 12.- Total temperature-velocity relationship at Mach 19 nozzle exit. $\frac{T_w}{T_{t,\infty}} \approx 0.17$.

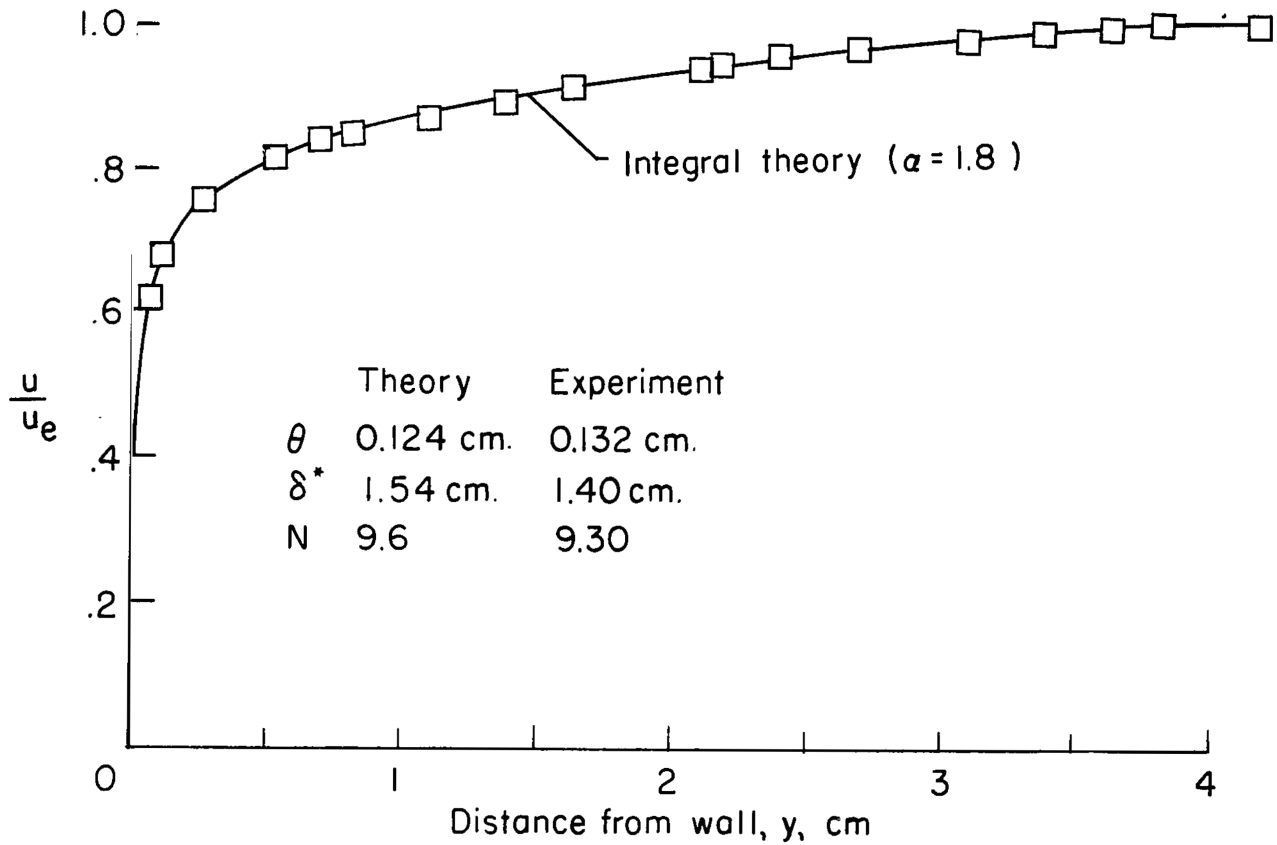

Figure 13.- Turbulent boundary-layer velocity profile at exit of Mach 6 contoured axisymmetric tunnel. $R_{e,\theta} = 3.8 \times 10^4$; $\frac{T_w}{T_{t,\infty}} = 0.66$.

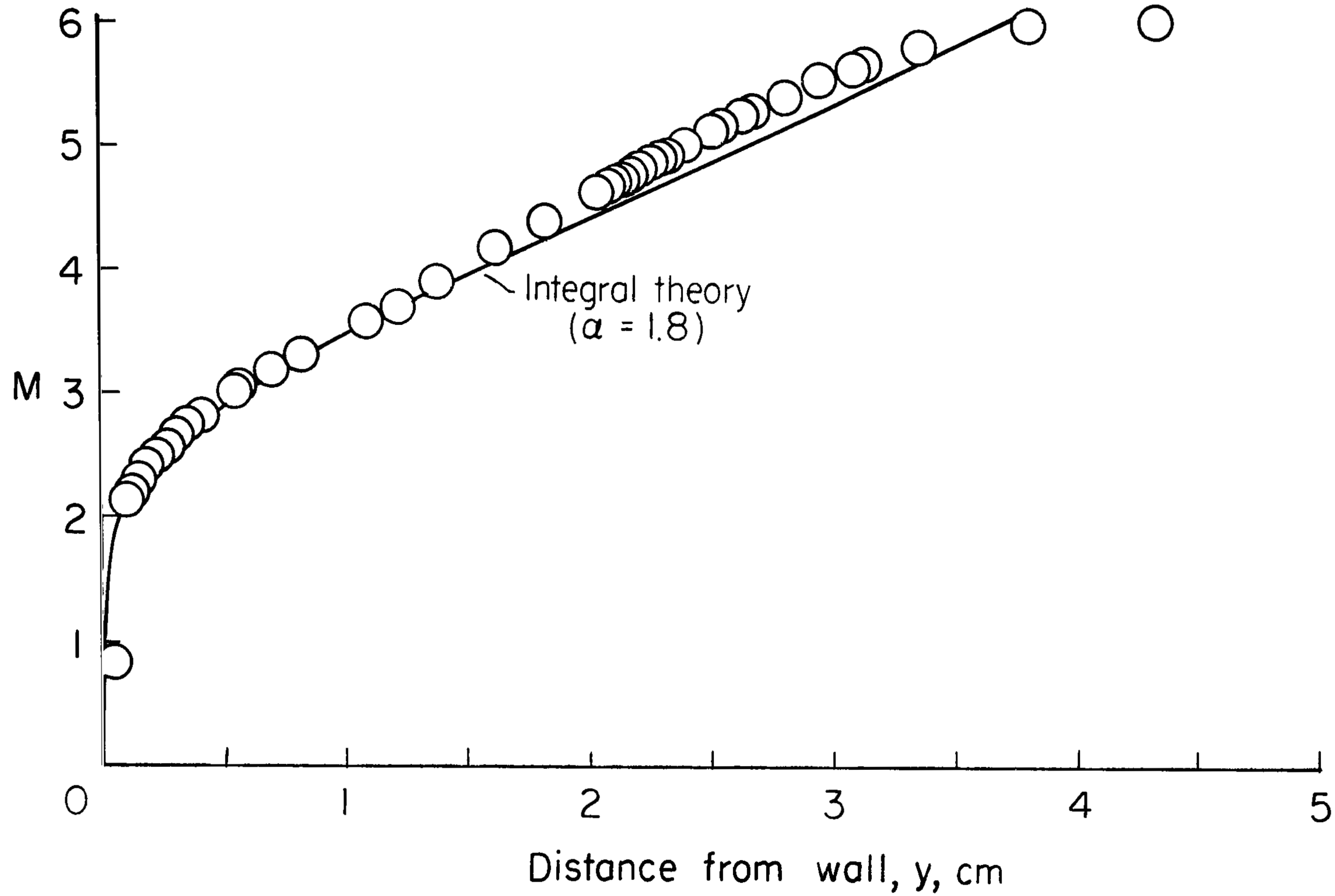

Figure 14.- Mach number profile at exit of Mach 6 nozzle. $R_{e,\theta} = 3.8 \times 10^4$; $\frac{T_w}{T_{t,\infty}} = 0.66$.

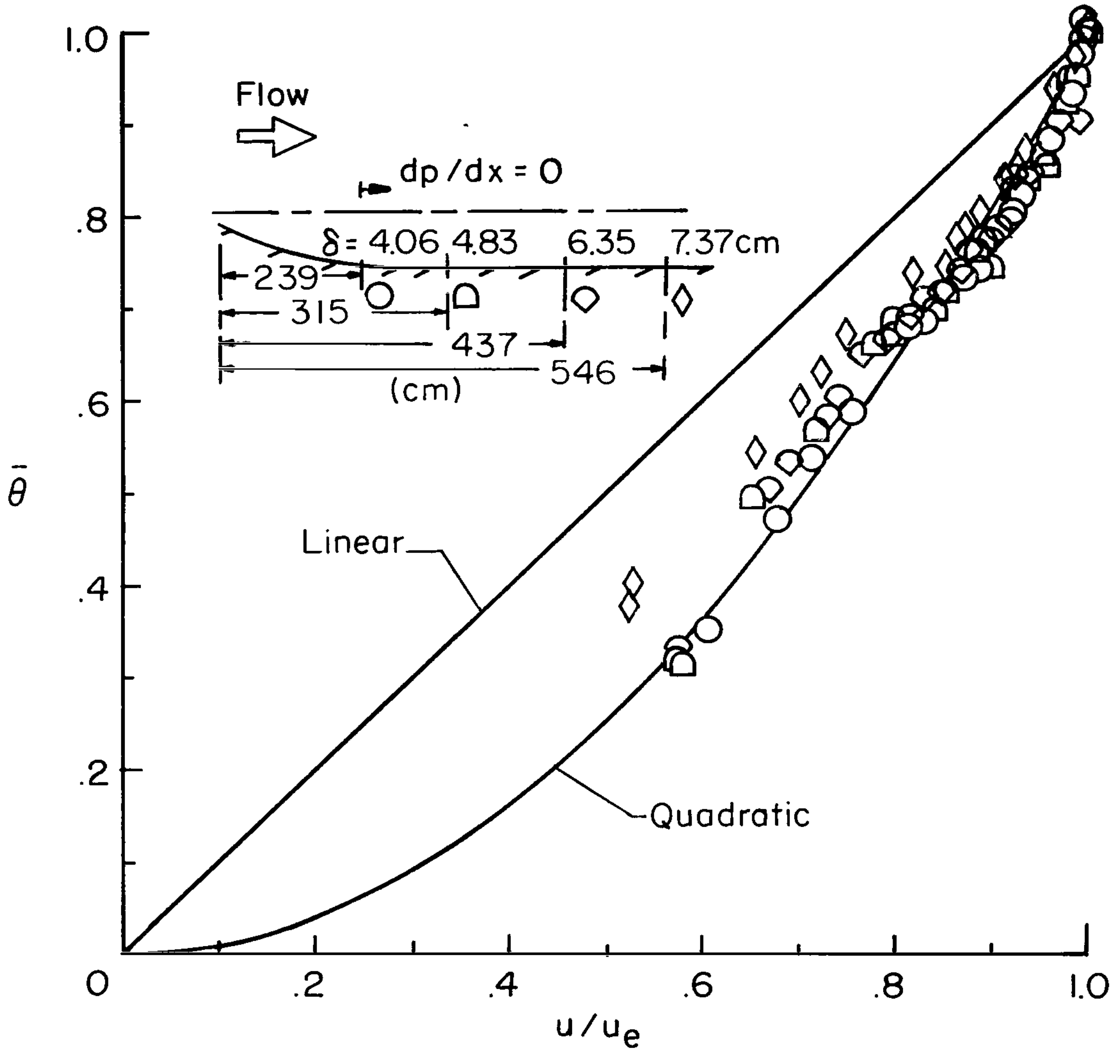

Figure 15.- Total temperature-velocity relationship at various distances downstream of Mach 6 nozzle throat. $\frac{T_w}{T_{t,\infty}} \approx 0.66$; $p_t \approx 40$ atmospheres.

NATIONAL AERONAUTICS AND SPACE ADMINISTRATION
WASHINGTON, D. C. 20546

OFFICIAL BUSINESS

FIRST CLASS MAIL

POSTAGE AND FEES PAID
NATIONAL AERONAUTICS AND
SPACE ADMINISTRATION

11L CC1 37 51 3CS 69226 00903
AIR FORCE WEAPCNS LABORAICRY/AFWL/
KIRTLAND AIR FORCE BASE, NEW MEXICO 8711

ATT E. LCU BOWMAN, ACTING CHIEF TECH. LI.

POSTMASTER: If Undeliverable (Section 158 Postal Manual) Do Not Return

"The aeronautical and space activities of the United States shall be conducted so as to contribute . . . to the expansion of human knowledge of phenomena in the atmosphere and space. The Administration shall provide for the widest practicable and appropriate dissemination of information concerning its activities and the results thereof."

— NATIONAL AERONAUTICS AND SPACE ACT OF 1958

NASA SCIENTIFIC AND TECHNICAL PUBLICATIONS

TECHNICAL REPORTS: Scientific and technical information considered important, complete, and a lasting contribution to existing knowledge.

TECHNICAL NOTES: Information less broad in scope but nevertheless of importance as a contribution to existing knowledge.

TECHNICAL MEMORANDUMS: Information receiving limited distribution because of preliminary data, security classification, or other reasons.

CONTRACTOR REPORTS: Scientific and technical information generated under a NASA contract or grant and considered an important contribution to existing knowledge.

TECHNICAL TRANSLATIONS: Information published in a foreign language considered to merit NASA distribution in English.

SPECIAL PUBLICATIONS: Information derived from or of value to NASA activities. Publications include conference proceedings, monographs, data compilations, handbooks, sourcebooks, and special bibliographies.

TECHNOLOGY UTILIZATION PUBLICATIONS: Information on technology used by NASA that may be of particular interest in commercial and other non-aerospace applications. Publications include Tech Briefs, Technology Utilization Reports and Notes, and Technology Surveys.

Details on the availability of these publications may be obtained from:

SCIENTIFIC AND TECHNICAL INFORMATION DIVISION

NATIONAL AERONAUTICS AND SPACE ADMINISTRATION

Washington, D.C. 20546